

# **The Intelligent ICU Pilot Study: Using Artificial Intelligence Technology for Autonomous Patient Monitoring**

**Anis Davoudi, MS<sup>1</sup>, Kumar Rohit Malhotra, BS<sup>2</sup>, Benjamin Shickel, MS<sup>2</sup>, Scott Siegel, MS<sup>1</sup>, Seth Williams, BS<sup>3</sup>, Matthew Ruppert<sup>1</sup>, Emel Bihorac, BS<sup>4</sup>, Tezcan Ozrazgat-Baslanti, PhD<sup>3,5</sup>, Patrick J. Tighe, MD MS<sup>6</sup>, Azra Bihorac, MD MS<sup>3,5</sup>, Parisa Rashidi, PhD<sup>1, 2, 5</sup>**

1 Department of Biomedical Engineering, College of Engineering, University of Florida, Gainesville, FL, USA

2 Department of Computer and Information Science and Engineering, University of Florida, Gainesville, FL, USA

3 Department of Medicine, College of Medicine, University of Florida, Gainesville, FL, USA

4 Department of Counselor Education, College of Education and human Performance, University of Central Florida, Orlando, FL, USA

5 Precision and Intelligent Systems in Medicine (Prisma<sup>P</sup>), University of Florida, Gainesville, FL, USA

Short title: Intelligent ICU

6 Department of Anesthesiology, College of Medicine, University of Florida, Gainesville, FL, USA

**Keywords:** Intelligent ICU, Delirium, Pervasive Monitoring, Wearable Sensors, Patient Face Recognition, Patient Expression Recognition, Patient Posture Classification, Patient Activity Intensity Patterns, ICU Environment Monitoring

## **Abstract:**

Currently, many critical care indices are not captured automatically, rather are repetitively assessed and recorded by overburdened nurses, e.g. physical function or facial pain expressions in nonverbal patients. In addition, many essential information on patients and their environment are not captured at all, or are captured in a non-granular manner, e.g. sleep disturbance factors such as bright light, loud background noise, or excessive visitations. In this pilot study, we examined the feasibility of using pervasive sensing technology and artificial intelligence for autonomous and granular monitoring of critically ill patients and their environment in the Intensive Care Unit (ICU). As an exemplar prevalent condition, we also characterized delirious and non-delirious patients and their environment. We used wearable sensors, light and sound sensors, and a high-resolution camera to collect data on patients and their environment. We automatically analyzed collected data using deep learning and statistical analysis. Our system performed face detection, face recognition, facial action unit detection, head pose detection, facial expression recognition, posture recognition, actigraphy analysis, sound pressure level detection, light level detection, and visitation frequency detection. We were able to correctly detect patient's face (Mean average precision (mAP) = 0.94), recognize patient's face (Mean average precision (mAP) = 0.80), and recognize their postures (F1= 0.94). We also found that all facial expressions, 11 activity features, visitation frequency during the day, visitation frequency during the night, light levels, and sound pressure levels during the night were significantly different between delirious and non-delirious patients (p-value<0.05). In summary, we showed that granular and autonomous monitoring of critically ill patients and their environment is feasible and can be used for characterizing critical care conditions and related environment factors.

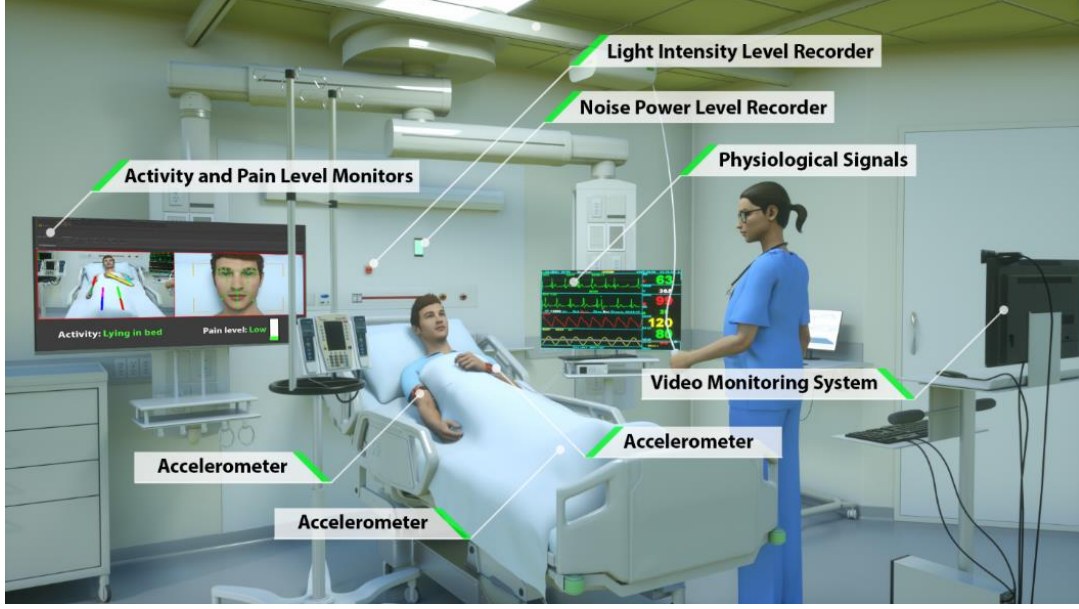
## Introduction

Every year, more than 5.7 million adults are admitted to intensive care units (ICU) in the United States, costing the health care system more than 67 billion dollars per year [1]. Currently, a wealth of information is recorded on each patient in the ICU, including high-resolution physiological signals, various laboratory tests, and detailed medical history in electronic health records (EHR) [2]. Nonetheless, important aspects of patient care are not yet captured in an automated manner. For example, while factors such as loud background noise, intense room light, and excessive rest-time visits contribute to sleep disruption and delirium [3], they are not currently measured. Additionally, many other aspects such as patient's pain facial expressions or functional status [4, 5] are not captured in a continuous and granular manner, as they require self-report, or require repetitive observations by ICU nurses [6, 7]. It has been shown that self-report and manual observations can suffer from subjectivity, poor recall, limited number of administrations per day, and high staff workload. This lack of granular and continuous monitoring can prevent timely intervention strategies [8-13].

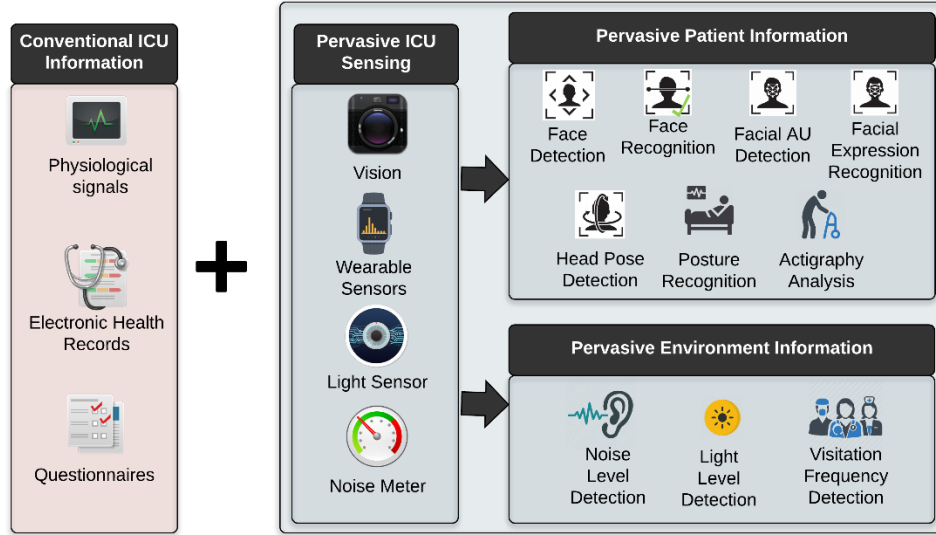
With recent advancements in artificial intelligence (AI) and sensing, many researchers are exploring complex autonomous systems in real-world settings [14]. In critical care settings, AI technology can assist in administering repetitive patient assessments in real-time, thus potentially enabling more timely interventions [15-17]. AI in critical care setting also can reduce nurses' workload, allowing them to spend time on more critical tasks.

In this study, we examined how pervasive sensing technology and AI can be used for monitoring patients and their environment in the ICU. We utilized three wearable accelerometer sensors, a light sensor, a sound sensor, and a high-resolution camera to capture data on patients and their environment in the ICU (Figure 1). We used computer vision and deep learning techniques to recognize patient's face, posture, facial action units, facial expressions, and head pose from video data. We also analyzed video data to find visitation frequency by detecting the number of visitors or medical staff in the room. To complement vision information for activity recognition, we analyzed actigraphy data from wearable accelerometer sensors worn on the wrist, ankle, and arm. Additionally, we captured room's sound pressure levels and light intensity levels to examine their effect on patients' sleep quality. The Freedman Sleep Questionnaire [18] was administered daily as the gold standard for assessing sleep quality. We also retrieved detailed clinical and physiological information from EHR for recruited patients (Table 1, Supplement). As an exemplar condition, Intelligent ICU was evaluated in the context of characterizing delirium patients and their environment. The Confusion Assessment Model-Intensive Care Unit (CAM-ICU) [19] was administered daily as the gold standard for detecting delirium.

The rest of the paper is as follows. We will demonstrate the results in section 2. Then, we will discuss the results in section 3. The methods will be covered in more details in section 4.



(a)



(b)

Figure 1 (a) Intelligent ICU uses pervasive sensing for collecting data on patients and their environment. The system includes wearable accelerometer sensors, video monitoring system, light sensor, and a sound sensor. (b) The Intelligent ICU information complements conventional ICU information. Pervasive information is provided by performing face detection, face recognition, facial action unit detection, head pose detection, facial expression recognition, posture recognition, actigraphy analysis, sound pressure level, detection, light level detection, and visitation frequency detection

## Pilot Study Results

We recruited 25 patients in the medical and surgical ICU at the University of Florida Health Shands Hospital (Table 1, Figure 1, Supplement). Eight patients (32%) were delirious for at least one day during their enrollment period, identified by the daily CAM-ICU assessment [19]. All delirious patients were identified as hyperactive by the Delirium Motor Subtyping Scale (DMSS-4) [20]. During the enrollment period, data was collected continuously for up to seven days from each patient. We collected 33,903,380 video frames containing at least one individual face, 16,123,925 video frames of patient posture, and 3,203,153 of patient facial expressions. We also collected 1,008 hours of accelerometer data, 768 hours of

sound pressure level data, and 456 hours of light intensity level data. Occasionally, one or more sensors were removed at patient’s request, during bathing, or during clinical routines. For training our deep learning models on ground truth labels, we annotated 65,000 video frames containing individual faces, and 75,697 patient posture video frames. All model training and testing was performed on an NVIDIA Titan X Pascal Graphical Processing Unit (GPU).

*Table 1. Cohort characteristics. Abbreviations: BMI: Body Mass Index, IQR: Inter-quartile Range, APACHE II: Acute Physiology and Chronic Health Evaluation II, ICU: Intensive Care Unit, LOS: Length of Stay. Initial cohort size: 25, final cohort size: 11.*

	All Participants (N=11)	Non-delirious (N=7)	Delirious (N=4)	p- value
Age, median (IQR)	62.50 (43.2, 70.0)	61.00 (37.5, 66.5)	59.50 (51.7, 67.7)	0.53
Female, Number (%)	2 (18.2)	1 (14.3)	1 (25)	1
Race, (%)				1
- White	10 (90.9)	6 (85.7)	4 (100)	
- African American	1 (9.1)	1 (14.3)	0 (0)	
BMI, median (IQR)	26.05 (24.5, 30.5)	26.18 (25.0, 28.7)	24.8 (22.1, 27.4)	0.65
Primary Diagnosis, Number (%)				0.50
- Neoplasms	1 (9.0)	1 (14.2)	0 (0.0)	
- Diseases of the circulatory system	2 (18.2)	2 (28.6)	0 (0.0)	
- Diseases of the digestive system	4 (36.4)	2 (28.6)	2 (50.0)	
- Injury, poisoning and certain other consequences of external causes	4 (36.4)	2 (28.6)	2 (50.0)	
APACHE II, median (IQR)	23 (19, 33)	21 (18, 27)	29 (23.25, 36.75)	0.14
Number of comorbidities, median (IQR)	2 (0, 4)	2 (1, 4)	1 (0, 3)	0.40
ICU LOS, median (IQR)	11.0 (7.6, 17.2)	11.0 (7.6, 20.1)	12.9 (9.1, 16.4)	1
Hospital LOS, median (IQR)	19.0 (16.0, 23.7)	19.0 (15.0, 22.5)	19.5 (16.0, 22.2)	1

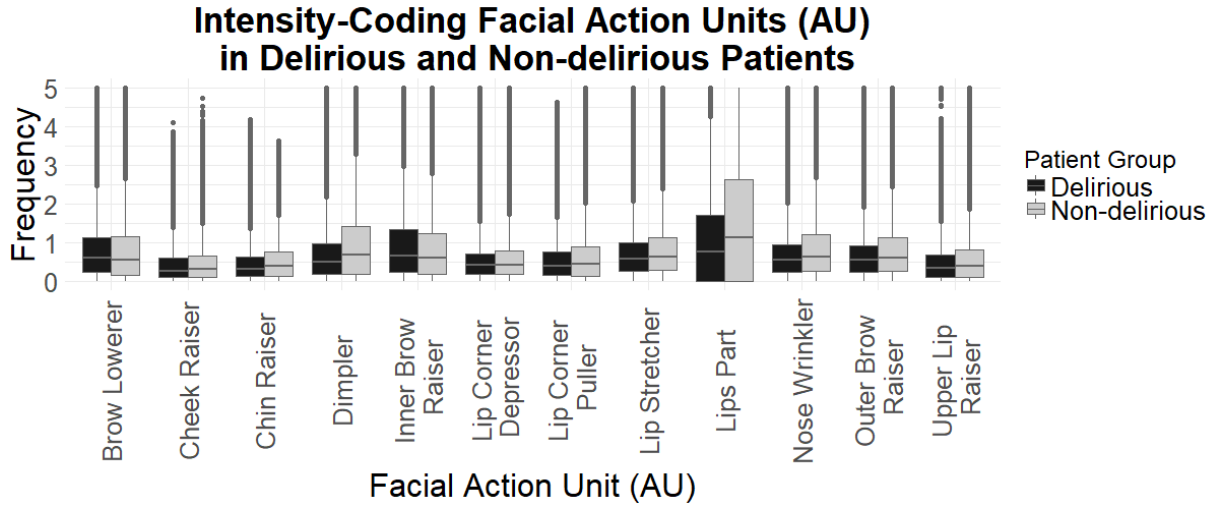
**Face Detection.** To detect all individual faces in each video frame (including patient, visitors, and clinical staff), we used the pretrained Joint Face Detection and Alignment using Multi-Task Cascaded Convolutional Network (MTCNN) [21]. Face detection was evaluated on 65,000 annotated frames containing at least one individual face, resulting in a Mean Average Precision (mAP) value of 0.94.

**Patient Face Recognition.** To recognize patient face among detected faces, we implemented the FaceNet algorithm [22] as an Inception-ResNet v1 model [23]. We achieved a mAP value of 0.80 for recognizing all patient faces, a mAP value of 0.75 for recognizing delirious patients, and a mAP value of 0.82 for recognizing non-delirious patients.

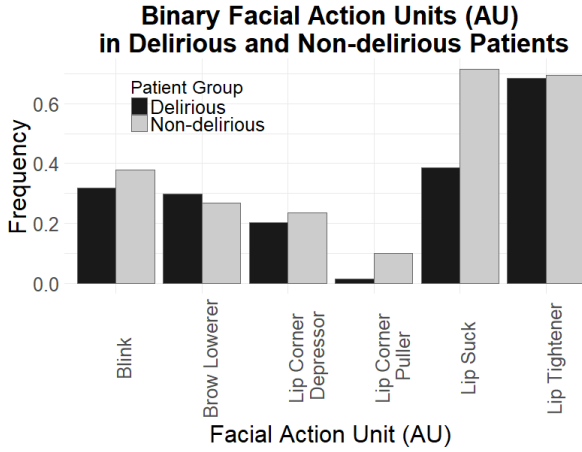
**Patient’s Facial Action Unit Detection.** We detected 18 facial action units (AUs) from 3,203,153 video frames using the pretrained OpenFace deep neural network [24]. The 18 AUs included six binary AUs (0 = absent, 1 = present), and 12 intensity-coding AUs (0 = trace, 5 = Maximum value). If at least one AU was detected, it was indicated as successful detection. Successful detection was achieved for 2,246,288 out of 3,203,153 video frames, with an average confidence of 0.88. The 18 detected AUs were compared between the delirious and non-delirious patients (Figures 2.a-b). All six binary AUs and all intensity-coding AUs were shown to be significantly different between the two groups (p-value<0.01).

**Facial Expression Recognition.** We used the Facial Action Coding System (FACS) to identify common facial expressions from their constituent AUs (Table 2, Supplement). Eight common expressions were considered, including pain, happiness, sadness, surprise, anger, fear, disgust, and contempt. The occurrence rate of facial expressions were compared between the delirious and non-delirious patients (Figure 2.c). Non-delirious patients exhibited significantly higher occurrence rate of pain expressions, concurring with their higher self-reported verbal pain scores [25]. All facial expressions had significantly different distribution among the delirious and non-delirious patients (p-value<0.01).

a)



b)



c)

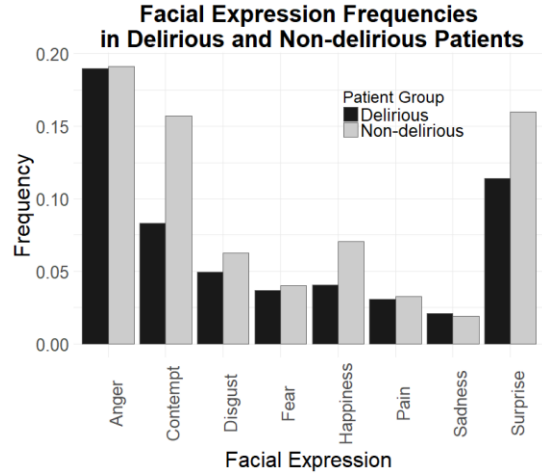


Figure 2 a) Distribution of intensity-coding facial AUs among delirious and non-delirious patients. Facial AUs are coded between 0 (absence of the facial AU) to 5 (maximum intensity of facial AU); b) Relative expression frequency of binary facial AUs (absent or present) among delirious and non-delirious patients during their enrollment period. The relative frequency shows how often a certain expression is observed in all recorded video frames; c) Relative frequency of facial expressions among the delirious and non-delirious patients, calculated based on constituent AUs.

**Head Pose Detection.** We detected three head poses including yaw, pitch, and roll, using the pretrained OpenFace deep neural network tool [24]. The head rotation in radians around the Cartesian axes were compared between the delirious and non-delirious patients, with the left-handed positive sign convention, and the camera considered as the origin. Delirious patients exhibited significantly less variation in roll head pose (rotation in-plane movement), in pitch head pose (up and down movement), and in yaw head pose (side to side movement) compared to the non-delirious patients (Figure 3.a).

**Posture Recognition.** To recognize patient posture, we used a multi-person pose estimation model [26] to localize anatomical key-points of joints and limbs. Then we used the lengths of body limbs and their relative angles as features for recognizing lying in bed, standing, sitting on bed, and sitting in chair. We obtained an F1 score of 0.94. The highest misclassification rate (11.3%) was obtained for *sitting on chair* misclassified as *standing*. The individual classification accuracy of recognizing postures was: sitting = %99.2, sitting on bed = %96.1, sitting on chair = 86.5%, and standing = 99.1% (Table 3, Supplement).

Delirious and non-delirious patients spent significantly different amount of time in different postures (p-value<0.05 for all four postures, Figure 3.b).

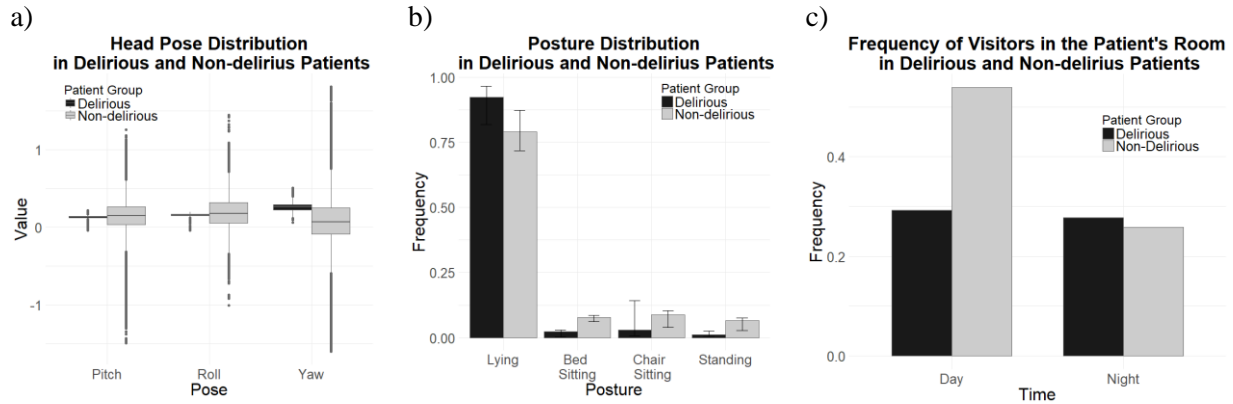


Figure 3 a) Distribution of head poses among delirious and non-delirious patients during their enrollment days. Pitch, yaw, and roll describe the orientation of the head in its three degrees of freedom. Pitch is the rotation around the right-left axis, up and down, as shaking the head “Yes”. Roll is rotation around the inferior-superior axis, rotation, as shaking the head “No”. Yaw is rotation around the anterior-posterior axis, side to side, like shaking the head “Maybe”; b) Percentage of the time delirious and non-delirious patients spent in each posture; c) The difference in frequency of disruptions for delirious and non-delirious patients during the day (7AM-7PM) and during the night (7PM-7AM). Frequency of disruption shows relatively how often a patient is disrupted, where disruption = 1.0 indicates being disrupted all the time, and disruption = 0.0 indicates no disruptions.

**Actigraphy Analysis:** We performed actigraphy analysis for the three accelerometr sensors worn on patient’s wrist, ankle, and arm, and compared the results between delirious and non-delirious patients. For the purpose of feature calculation, we consider daytime from 7AM to 7PM, and nighttime from 7PM to 7AM, based on nursing shift transitions. Figure 4.a-c show the smoothed accelerometer signal avergaed over all delirious and all non-delirious patients (Figures 7.a = wrist, 7.b = arm, 7.c = ankle). We also derived 17 actigraphy features per each accelerometer (Table 2), resulting in 51 total features for the wrist, ankle, and arm senhors. We compared actigraphy features in delirious and non-delirious patients for the wrist-worn sensor, arm-worn sensor, and ankle-worn sensor (Table 2, Table 7-8, Supplement).

Delirious patients had higher mean and higher standard deviation activity for the entire 24-hours cycle, daytime (7am-7pm), and nighttime (7pm-7am). The difference between root mean square of sequential differences/standard deviation (RMSSD) of delirious and non-delirious patients was statistically significant, a sign of the higher presence of nonintentional wrist movements of the delirious patients. The 10-hour window with maximum activity intensity showed different levels of activity between the two patient groups. However, activity in the 5-hour window with the lowest activity intensity was not significantly different, possibly due to low activity levels in ICU in general. The number of immobile moments during the day and during the night were also different between the two groups, with less number of immobile moments detected for the delirious patients, hinting at their restlessness and lower sleep quality. The differences in actigraphy features are reflected in the BRADEN scores related to activity and mobility. Several Braden components including activity, mobility, and friction and shear, which reflects on requiring help to move-, were significantly different between delirious and non-delirious patients. However, total Braden score was not significantly different between delirious patients and non-delirious patients (Table 4, Supplement).

## Sensor Data and Physiological Data in Delirious and Non-delirious Patients

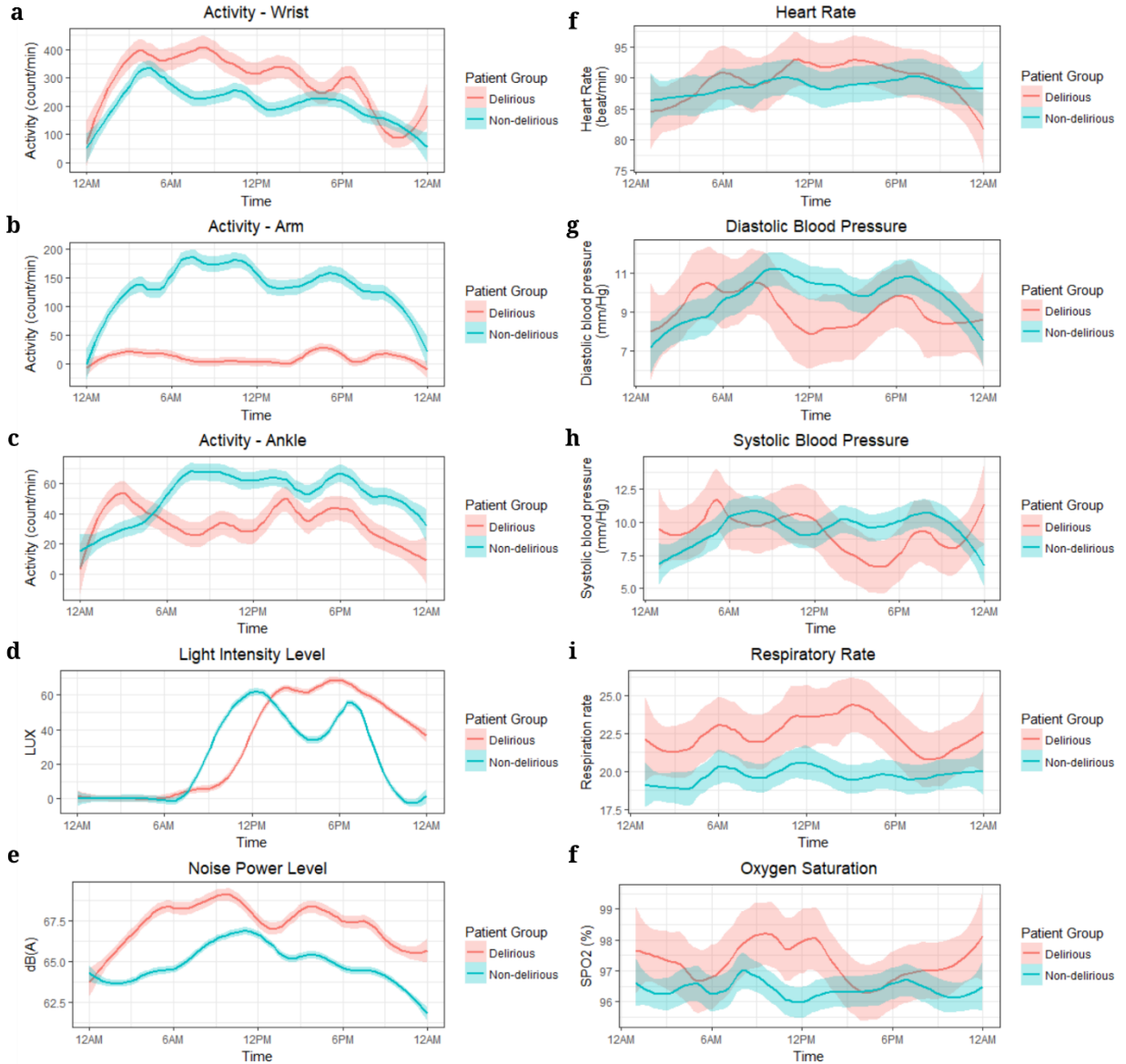


Figure 4 Delirious and non-delirious group comparisons for a-e) sensor data and f-j) physiological data. Sensor data included accelerometer data recorded using actigraphs on the wrist, arm, and ankle, as well as light intensity level recorded using an actigraph capable of recording light intensity level and the sound pressure level using an iPod on the wall behind the patient's bed. Physiological data included heart rate, systolic blood pressure and diastolic blood pressure, respiration rate, and oxygen saturation. Physiological data were collected with a resolution of approximately once per hour as part of the patient's care. The graphs show the smoothed average value per group, with the transparent band around each average line showing the 95% confidence interval.

Table 2. Actigraphy features for the **wrist**, compared between the delirious and non-delirious groups. M10: activity level during the 10-hour window with the highest sum of activity, L5: activity level during the 5-hour window with the lowest sum of activity. Relative amplitude:  $(M10-L5)/(M10+L5)$ . RMSSD: Root mean square of sequential differences. RMSSD/SD: root mean square of sequential differences/standard deviation. Immobile minutes are minutes with zero activity.

	Non-delirious (N=15)	Delirious (N=5)	p-value
Mean of activity for whole day, median (IQR)	53.9 (19.5, 161.6)	332 (251, 457.6)	<b>0.01</b>
Mean of activity for daytime	69.7 (16.7, 198.1)	347.4 (318.9, 384.8)	<b>0.03</b>
Standard deviation of activity for daytime	246.8 (99.3, 472.5)	640.6 (487.5, 697.2)	<b>0.05</b>
Mean of activity for nighttime	46.4 (22.8, 94.7)	332.3 (310.7, 541.8)	<b>0.008</b>
Standard deviation of activity for nighttime	192.5 (130.5, 313.3)	664.1 (469.1, 930.9)	<b>&lt;0.01</b>
Activity of 10-hour window with highest sum of activity (M10)	60137.3 (15029.5, 176498.3)	282918.1 (254729.3, 457448)	<b>&lt;0.01</b>
Time of M10	318 (157, 574)	275 (47, 627)	1
Time of M10 (hour)	6 (3, 9)	5 (1, 11)	1
Activity of 5-hour window with lowest sum of activity (L5)	3916.7 (1195.7, 10236.2)	44163.2 (1949.3, 54779.3)	0.35
Time of L5	298 (176, 959)	1067 (212, 1119)	0.36
Time of L5 (hour)	5 (3.5, 16.5)	18 (4, 19)	0.36
Relative amplitude	0.9 (0.7, 0.9)	0.9 (0.8, 1)	0.61
Standard deviation of activity for whole day	199.9 (116.3, 456.3)	558.4 (523.1, 826.4)	<b>0.02</b>
RMSSD	223.4 (137.3, 469.7)	538.7 (487.4, 730.2)	<b>0.04</b>
RMSSD/SD	1.1 (1.0, 1.2)	0.9 (0.9, 1)	<b>&lt;0.01</b>
Number of immobile minutes during the day	564 (416, 654)	345 (200, 384)	<b>0.02</b>
Number of immobile minutes during the night	602 (580, 650)	344 (314, 374)	<b>0.01</b>

**Visitation Frequency.** The pose estimation model was also used to identify the number of individuals present in the room at any given time, including visitors and clinical staff. Delirious patients on average had fewer visitor disruptions during the day, but more disruptions during the night (Figure 3.c).

**Room Sound Pressure Level.** The sound pressure levels for delirious patients' rooms during the night were on average higher than the sound pressure levels of non-delirious patients' rooms (Figure 4.e). Average nighttime sound pressure levels were significantly different between the delirious and non-delirious patients ( $p$ -value<0.05).

**Room Light Intensity.** Delirious patients on average experienced higher light intensity during the evening hours, as can be seen in Figure 4.d. Average nighttime light intensity levels were significantly different between the delirious and non-delirious patients ( $p$ -value<0.05).

**Sleep characteristics:** We examined the Freedman Sleep Questionnaire [18] responses for the delirious and non-delirious patients to compare their sleep patterns. While the median of overall quality of sleep in the ICU and effect of acoustic disruptions and visitations during the night were different among the delirious and non-delirious groups, these differences were not statistically significant. However, delirious patients reported a lower overall ability to fall asleep compared to non-delirious patients, and they were more likely to find the lighting to be disruptive during the night ( $p$ -value= 0.01,  $p$ -value=0.04, respectively, Figure 2, Supplement).



**Physiological and EHR data:** Delirious patients on average had higher average heart rate, oxygen saturation, and respiration rate, a sign of potential respiratory distress. Systolic and diastolic blood pressure of the delirious patients were lower than non-delirious patients during the evenings (Figure 4.f-4.j). Among the five patients with more than one delirious days and 10 patients with all non-delirious days, all the delirious patients had enteral feeding orders, while 40% of non-delirious patients had enteral feeding order during their enrollment days. Patients' demographic and primary diagnosis were not significantly different between the delirious and non-delirious patients (Table 1).

## Discussion

In this study, we showed the feasibility of pervasive monitoring of patients in the ICU. We performed face detection, face recognition, facial action unit detection, head pose detection, facial expression recognition, posture recognition, actigraphy analysis, sound pressure level detection, light level detection, and visitation frequency detection, in the ICU. This is the first study to develop an autonomous system for patient monitoring in the ICU. The main purpose of the study was mainly to demonstrate the possibility of pervasive monitoring of ICU patients to capture aspects of their stay in the ICU that have not been captured to date. As an example, we evaluated our system for characterization of patient and ambient factors relevant to delirium syndrome [3, 27, 28]. Such a system can be potentially used for detecting activity and facial expression patterns seen more commonly in delirious patients. It also can be used for predicting delirium risk based on environment conditions such as room sound pressure level and light intensity which are known to correlate with delirium [29-33]. This system can be built with an estimated cost of < \$300 per ICU unit, a relatively low cost compared to daily ICU costs of thousands of dollars per patient. It should be noted that after proper cleaning procedures, the same devices can be also reused for other patients, further reducing the amortized cost per patient in the long term.

**Circadian Rhythm.** Our collected data hint at several interesting observations, including more significant disruption of circadian rhythm of physical activity in delirious patients, as confirmed by other studies [34-36]. To concur with existing practice in literature, we used standard sleep quality questionnaires to capture the patients' sleep quality and the effect of environmental and clinical disruptions. To identify delirium, we used the standard CAM-ICU assessment as gold standard in the ICU. Compared to previous studies, we collected and analyzed information at a granularity and with an accuracy that is impossible to obtain using conventional methods such as questionnaires. Circadian rhythm, which is important for many health regulatory processes in the body, is generally severely disrupted in ICU patients [34-36]. Delirious patients reported lower overall ability to fall asleep in the ICU. Delirious patients also reported a higher degree of disruption from lighting compared to non-delirious patients. Their noise perception was not statistically significantly different from the non-delirious group, even though the average sound pressure level from the delirious patients' rooms was higher than that of the non-delirious patients' rooms, possibly due to affected hearing and vision perception of delirious patients.

**Facial Expressions and Head Pose.** Prior literature shows discriminative power of individual AUs for affect valence [37]. We were able to show that distributions of several facial AUs are different among the delirious and non-delirious groups. The differences in the distribution of such AUs point to the differences in affections of delirious and non-delirious patients. For instance, presence of inner brow raiser AU signals a negative valence [37], and is stronger among the delirious patients than non-delirious patients (Figure 2). Extended range of head poses in non-delirious patients compared to delirious patients (Figure 3.a) might be the result of more communication and interaction with the surrounding environment.

**Actigraphy Analysis.** We additionally extracted several statistical features to better examine the actigraphy information. Several wrist-based actigraphy features show significant differences between delirious and non-delirious patients, including higher mean and standard deviation activity for delirious patients. This was expected since our delirious patients consisted of hyperactive subtype. The significant difference between wrist RMSSD of delirious and non-delirious patients can be a sign of nonintentional hand movements in delirious patients due to agitation. The actigraphy features did not show significant difference

for arm and ankle (Table 7-8, Supplement). This might stem from the overall limited body movements of all ICU patients. This insight can potentially be used reduce the number of required on-body sensors for monitoring specific conditions such as delirium. To the best of our knowledge, this is the first study that examines the wear location for actigraphy devices in characterizing activity patterns in delirium patients. It should be noted that the ideal location for wearing the actigraphy device is not necessarily the same for different clinical conditions [38-40]. The wrist-based actigraphy features can be potentially used in delirium detection, as well as in tracking efficacy of interventions.

**Visitation Frequency.** Using our vision techniques, we were also able to observe differences in visitor disruptions among delirious and non-delirious patients. More disruptions were observed during the day for non-delirious patients. This may both contribute to and stem from delirium, since interactions with others can have reorientation effects and reduce risk of delirium. At the same time, since delirious patients do not engage in interactions with others, they might have shorter visitations from both family and clinical staff. More disruptions during the day for non-delirious patients possibly points to their capability to have more interactions with others, including family caregivers and visitors. ICU environment instills a sense of loneliness in the patients, reported by many delirious patients [41-44]. Visitations during the day may contribute to preventing delirium, because of conversations' reorientation effects and the sense of relief that seeing recognizable faces invokes. On the other hand, isolation precautions have been reported to up to double the rate of delirium [45-47]. Delirious patients also had more disruptions during the night, possibly due to their more severe condition and frequent visits from providers, which could aggravate their sleep disruptions.

While our system shows great promise for future ICU patient monitoring applications, there are several limitations that need to be considered. As a pilot study to assess the feasibility of the system, we recruited a small number of patients. This could possibly affect some of the results and their variability, once examined in a larger cohort. For example, we did not detect any significant differences between actigraphy features derived from ankle and arm sensors, but larger sample size and more diverse features might show higher discriminative power. Using a larger sample size would also allow us to better customize our deep learning vision models to the ICU environment.

Another limitation of the study is that we did not consider the medications that patients were receiving during their stay in the ICU. Sedatives, analgesics, and anticholinergic medications may potentially affect patients' sleep, pain, activity patterns, and delirium. To correctly account for these factors, the drugs' dosages and half-times need to be extracted and their continuous effect on each individual patient need to be considered.

Implementing our system in a real ICU also poses many challenges, resulting in several limitations in our study. One major issue is the crowded scene in the ICU room, resulting in patient face occlusion and inability to detect expressions at all times. One potential solution is deploying multiple cameras with different view angles. Patient's face and body might be also obstructed by ventilation devices, bandage, or simply blocked from view by blankets. Another issue rises from the multitude of medical devices on the patient, making it difficult to use wearable sensors on all patients. A related issue occurring for the wearable sensors is that they might get lost, or the clinical staff might not place them in the right location after taking them off for a bath.

Another challenge was in accurate environment data collection, stemming from the physical properties of light waves. While we made every effort to place the light sensor near the patient's head to record the same amount of light exposure that the patient is experiencing, individuals or medical equipment might block the light sensor. Again, deploying multiple light sensors, as well as developing vision-based light analysis modules can alleviate this problem.

Privacy can be also a major concern for any system that uses video monitoring. To be able to develop and validate our system, we needed to annotate the video frames to establish ground truth for every event -face

recognition, posture detection, and disruptions. However, a future operational version can rely on real-time and online vision analysis without storing any video data. This approach could also reduce the need for extensive storage requirements.

In summary, as a proof of concept, we were able to demonstrate the possibility of pervasive monitoring of patients in the ICU. We expect future similar systems can assist in administering repetitive patient assessments in real-time, thus potentially enabling more timely interventions, reducing nursing workload [15-17], and opening new avenues for characterizing critical care conditions on a much more granular level.

## **Materials and Methods**

This study was carried out at surgical and medical ICUs in the Shands Hospital, Gainesville, Florida. It was approved by University of Florida Institutional Review Board. Written informed consent was obtained from patients and/or their surrogates before enrollment in the study. Exclusion criteria included: 1) anticipated ICU stay of less than one day, 2) age <18 years, and 3) inability to wear an ActiGraph. For each patient, data was collected for up to one week, or until discharge or transfer from the ICU, whichever occurred first.

Among consenting patients, one patient withdrew before data collection started, one was excluded because of being transferred from the ICU before data collection commenced, one patient stayed for less than a day in the ICU, three patients' data were not useable because it was collected with an older non-compatible system. Five were not considered in the delirium analysis because they had both delirium and non-delirium days. Delirious patients (defined as patients who were delirious throughout their enrollment period, number of patients=four) and non-delirious patients (defined as patients who were not delirious at any day during their enrollment period, number of patients=7) did not differ in baseline characteristics (Table 1).

For characterizing delirium in terms of activity, facial expressions, environmental light and sound pressure levels, and disruption, delirious patients were defined as those who were delirious throughout their enrollment period, as detected by the CAM-ICU test. To better observe the differences between the delirious and non-delirious patients, we only compared the data between patients who were delirious throughout their enrollment period, and those who were non-delirious throughout their enrollment period.

## **Data Acquisition**

The pervasive sensing system for data acquisition included (1) a high-resolution and wide-field-of-view camera, (2) three wearable accelerometer sensors, (3) light sensor, (4) microphone for capturing sound pressure levels, and (4) a secure local computer. A touchscreen user-friendly interface allowed nurses and caregivers to stop data collection at any time. Data were captured on a local secure computer throughout the patient enrollment period and transferred to a secure server for analysis upon patient discharge.

**Vision:** We captured video using a camera with a 90° diagonal field of view with 10X optical zoom for zooming on patient face, and at 15 frames per seconds (fps) speed. The camera was placed against the wall, facing the patient. We took several privacy precautions with respect to video data, including posting clearly visible signs warning of “recording in session”. A sliding lens cover was used as a quick privacy alternative. No audio information beyond aggregate sound pressure levels was collected. A simple user interface also allowed the nurses and family caregivers to stop recording at any time, or to delete any scenes if needed.

**Wearable Sensors:** Wearable accelerometer sensors provide complementary information to vision information for activity recognition in the ICU. We used three Actigraph GT3X (GT3X) devices (ActiGraph, LLC. Pensacola, Florida) to record patients' activity intensity throughout their enrollment period. We placed one GT3X device on the patient's dominant wrist, one on the dominant arm, and another on the dominant ankle to be able to examine different lower and upper body movements. For patients with medical equipment on their dominant wrist, arm, or ankle, or those who did not wish to wear the device on any of these positions, we placed the GT3X device on the opposite side, or removed it altogether, if necessary. Nurses were instructed to remove the devices for bathing and medical procedures, if necessary,

and to replace the devices afterwards. The GT3X sensor weighs less than 19 grams and can record data for up to 25 days. It records activity intensity in form of activity counts [48]. We recorded data at 100Hz sampling rate and used 1-min activity counts in our analysis.

**Sound and Light:** To capture the effect of environment disruptions on sleep quality, we recorded light intensity and sound pressure levels in the room throughout the patient’s enrollment period.

**Physiological Signals and EHR Data:** We also retrieved physiological signals recorded in the ICU via bedside monitors, including heart rate, temperature, systolic and diastolic blood pressure, respiratory rate, and oxygen saturation. Additionally, we retrieved EHR information including demographics, and admission information such as diagnosis codes, lab results, and enteral feeding status.

**Questionnaires:** As gold standard, we administered daily questionnaires to assess patients’ sleep quality during their enrollment. We used the Freedman sleep questionnaire (Appendix A). We also administered the CAM-ICU delirium assessment daily. For patients who were asleep or unavailable because of clinical procedures, the questionnaires were administered as soon as they became available, before 3 pm.

## Analysis

Once data was captured by our pervasive sensing system, it was analyzed to examine different aspects of patient status and environment. We used vision information for face detection, face recognition, facial action unit detection, head pose detection, facial expression recognition, posture recognition, and visitation frequency detection. We employ several deep neural network algorithms for analyzing video data and we use statistical analysis to analyze accelerometer sensor data, as well as to compare the environment factors and activity intensity of the delirious and non-delirious patients. For numerical variables description, we used mean and standard deviation in case of approximately normal distribution. In case of variables with skewed distribution, we used median and inter quantile range (25<sup>th</sup>, 75<sup>th</sup>). We used Tensorflow: 1.1.0, Opencv: 3.2.0, Caffe: 1.0 for implementing vision algorithms. We used Scikit-learn: 0.18.1 and R: 3.4.1 for conventional machine learning and statistical analysis.

**Face Detection.** As a first step, we detected all individual present in the room. We used the Joint Face Detection and Alignment using Multi-Task Cascaded Convolutional Network (MTCNN) to detect individuals in each video frame. This framework employs a cascaded architecture with three stages of deep convolutional neural networks (CNN) to predict face and landmark locations in a coarse-to-fine manner (Figure 3, Supplement). We evaluated the accuracy of the MTCNN models based on ground truth provided by expert annotator. A total of 65,000 video frames were annotated by delineating a bounding box surrounding each individual.

**Face Recognition.** After individual faces were detected, we performed face recognition to identify the patient in each video frame. This step is necessary, since at any given moment several individuals can be present in the room, including the patient, nurses, physician, and visitors. To perform face recognition, we implemented the FaceNet algorithm, which consists of an Inception-ResNet V1 model. First, we extracted 7 seconds of still images at 15 fps containing the patient face, as training data. Training data was passed through the face detection pipeline. Thus, the input to FaceNet model is the set of aligned images obtained from MTCNN. The trained classifier for each patient was tested on 6,400 randomly selected images of the same patient, containing both patients and non-patients in the same frame. We evaluated the accuracy of the FaceNet model per each patient. If a patient was recognized with a probability of 0.9 or higher, it was reported as a positive recognition. Pipeline of the patient face recognition system is shown in Figure 5.a.

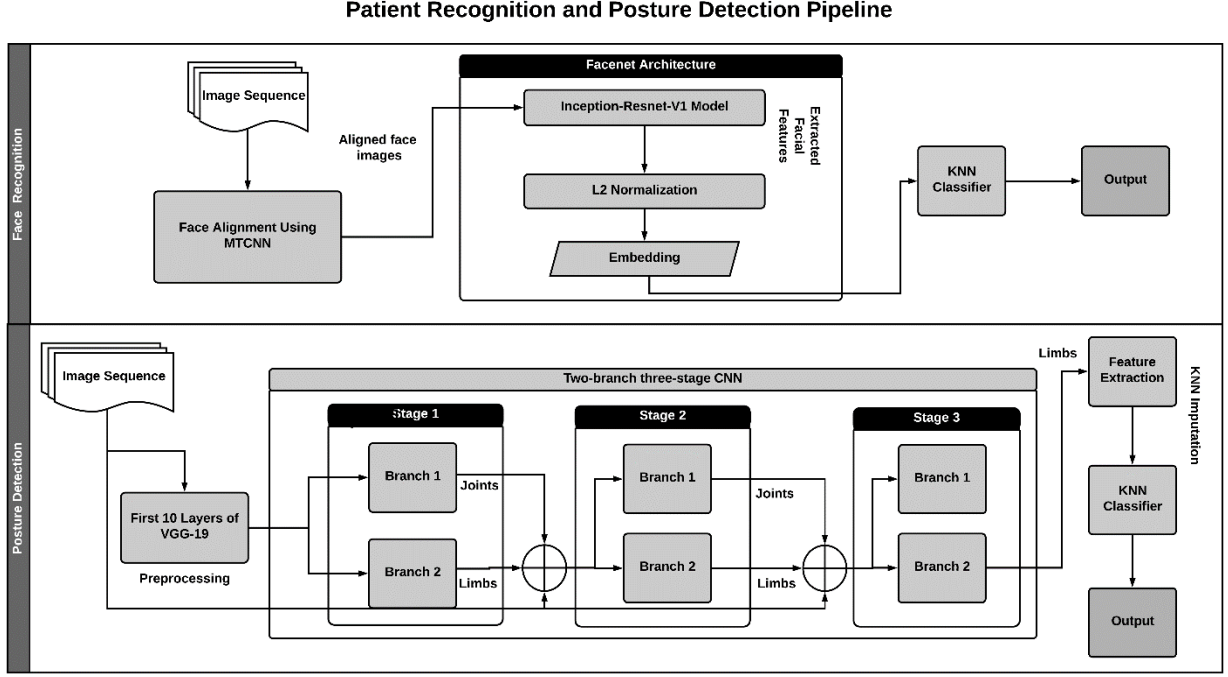


Figure 5 a) Pipeline of the patient recognition system begins with alignment of faces in the image using MTCNN (Multi-stage CNN). The aligned images are then provided as input to the faceNet network which extracts features using a pre-trained Inception-Resnet-V1 model, then performs L2 normalization on them, and finally stores them as feature embeddings. These embeddings are used as input for the k-nearest neighbor (KNN) classifier to identify posture. b) Pipeline of the posture recognition system includes a two-branch three-stage CNN and a KNN classifier. At each stage of the CNN, Branch 1 predicts the confidence maps for the different body joints, and branch 2 predicts the Part Affinity Fields for the limbs. These predictions are combined at the end of a stage and refined over the subsequent stage. After stage 3, the part affinity fields of limbs are used to extract the lengths and angles of the body limbs. Any missing values are imputed using the KNN imputation, and a pre-trained KNN classifier is used to detect posture from the extracted features.

**Facial Action Unit and Expression Recognition:** For each video frame, facial Action Units (AUs) were obtained from the OpenFace toolbox and were used to detect eight common facial expressions: pain, happiness, sadness, surprise, anger, fear, disgust, and contempt (Table 2, Supplement). Facial expressions were only considered during daytime (7am-7pm), when there is sufficient light in the room. Based on the FACS formulas (Table 2, Supplement), pain expression was identified as a combination of the following AUs: AU4 (brow lowerer), AU6 (cheek raiser), AU7 (lid tightener), AU9 (nose wrinkler), AU10 (upper lip raiser), and AU43 (eyes closed). Other facial expressions can be similarly identified. Once an expression was detected, we computed how often that expression  $e_i$  was observed, denoted as the expression frequency  $f_i$ . The relative expression frequency  $f_i$  is calculated as in Eq. 1. Here,  $N_i$  refers to the number of frames where expression  $e_i$  was observed, and  $N$  refers to total number of frames.

$$f_i = \frac{N_i}{N} \quad (1)$$

**Posture Classification:** After detecting and recognizing patient's face, we localized anatomical key-points of joints and limbs using the real-time multi-person 2D pose estimation [26] with part affinity fields (Figure 5.b). This allowed us to recognize poselets, which describe a particular part of posture under a given viewpoint [53]. The part affinity fields are 2D vector fields that contain information about the location and direction of limbs with respect to body joints. Our pose detection model consisted of two Fully Convolutional Neural networks (FCN) [51] branches, where one branch detects the locations of joints, and the other branch detects the association of those body joints as limbs. Identified poselets were provided to a k-nearest neighbor (KNN) classifier to identify the full posture. To train the model using a balanced

dataset, we augmented ICU patient data with scripted data (Appendix C). We considered four main posture classes to be recognized: lying in bed, standing, sitting on bed, and sitting on chair. Several ICU functional and mobility scales are based on evaluating patients' ability to perform these activities [52, 53].

**Actigraphy.** We calculated several statistical features to summarize the actigraphy data obtained from wrist, arm, and ankle. We used LOESS non-parametric regression method for smoothing to show the smoothed average of activity intensity for each group over the course of the day. We compared fifteen features extracted from the accelerometer data of the delirious and non-delirious patients. Features used in this analysis include four groups of features to reflect different aspects of activity intensity patterns. First group of features are mean and standard deviation (SD) of activity intensity for the whole day, during daytime, and during nighttime. Second group of features are activity intensity of 10-hour window with highest sum of activity intensity (M10), time of start of M10 window, activity intensity of 5-hour window with lowest sum of activity intensity (L5), time of start of L5 window, relative amplitude- which is  $(M10-L5)/(M10+L5)$ . Third group of features are Root Mean Square of Sequential Differences (RMSSD), RMSSD/SD. The fourth group of features are number of immobile minutes during daytime and during nighttime. Immobile minutes are defined as minutes with activity intensity of zero. Mean of activity intensity reflects the amount of patient's activity intensity, while standard deviation of activity intensity reflects the amount of change in patient's movement. M10 and L5, and their corresponding start times are chosen to show what times the most amount of activity, and the least amount of activity occur, and to detect whether they correspond to daytime and nighttime, respectively. RMSSD is used to detect immediate changes in the activity intensity, which can potentially point to unintentional activity, since patients in the ICU do not normally have fast actions for long periods of time, and RMSSD/SD normalizes these immediate changes by the overall changes in the data captured by standard deviation. Number of immobile minutes can be used to observe the percentage of the time patients were inactive during the day (undesirable) and during the night (desirable).

**Sound and Light:** We placed an iPod with a sound pressure level recording application and a GT3X with light sensor on the wall behind the patient's bed to record sound pressure levels and light intensity levels.

Sound pressure level collection was performed using the built-in microphone of the iPod. Sound waves can be described as a sequence of pressure changes in time domain, and ears detect changes in the sound pressure [54]. Sound pressure level (SPL) is a logarithmic measure of the effective pressure of a sound relative to a reference value and is measured in decibel (dB). Sound pressure is proportional to sound intensity and is defined as in Eq. 2.

$$SPL = \ln\left(\frac{p}{p_0}\right) N_p = 2 \log_{10}\left(\frac{p}{p_0}\right) B = 20 \log_{10}\left(\frac{p}{p_0}\right) dB \quad (2)$$

Here,  $p$  is the root mean square sound pressure,  $p_0$  is the reference sound pressure (commonly hearing threshold at 1KHz (0 dB)),  $1 N_p$  is the neper;  $1 N_p \approx 8.6858 dB$ . Table 5 Supplement gives examples of sound pressure levels [55].

GT3X has an integrated ambient light sensor that allows for the quantification of light intensity, reported in lux. A lux is a unit derived from the International System of Units used to assess illumination, a measure of light intensity at any point, and is equal to one Lumens per square meter. GT3X light sensor has a maximum value of 2500 lux, with estimate interpretation comparisons given in Table 6 Supplement [56].

**Visitation Frequency Detection.** For this purpose, we used the same model that was used for detection of poselets. Poselets were used for detecting the number of people present in the room, in each frame. In addition to the patient, a detected individual could be a visitor or a member of the clinical team. Presence of anyone other than the patient was considered as visitation. We compared the frequency of visitations for delirious and non-delirious patients during the day (7AM-7PM) and during the night (7PM-7AM).

## ACKNOWLEDGMENT

This work is supported by NSF CAREER 1750192 (PR), NIH/NIGMS P50 GM111152 (AB, TOB), NIH/NIA P30 AG028740 (PR), and NIH/NIGMS RO1 GM-110240 (PR, AB). The Titan X Pascal partially used for this research was donated by the NVIDIA Corporation.

### Author Contributions:

Study design: A.B. and P.R.; Data collection: M.R., S.W., E.B., and A.D.; Data analysis: A.D., K.R.M., B.S., S.S., and T.O.; Data interpretation: A.D., K.R.M., and P.J.T.; Drafting the manuscript: A.D. and P.R.; Critical revision of the manuscript: A.B. and P.R. all authors approved the final version of the manuscript to be published.

**Competing interests:** The authors declare no competing interests.

### REFERENCES

- [1] N. A. Halpern and S. M. Pastores, "Critical care medicine in the United States 2000-2005: an analysis of bed numbers, occupancy rates, payer mix, and costs," (in eng), *Crit Care Med*, vol. 38, no. 1, pp. 65-71, Jan 2010.
- [2] A. Jalali, D. Bender, M. Rehman, V. Nadkanri, and C. Nataraj, "Advanced analytics for outcome prediction in intensive care units," in *Engineering in Medicine and Biology Society (EMBC), 2016 IEEE 38th Annual International Conference of the*, 2016, pp. 2520-2524: IEEE.
- [3] B. G. Arenson, L. A. MacDonald, H. P. Grocott, B. M. Hiebert, and R. C. Arora, "Effect of intensive care unit environment on in-hospital delirium after cardiac surgery," *The Journal of thoracic and cardiovascular surgery*, vol. 146, no. 1, pp. 172-178, 2013.
- [4] J. Barr *et al.*, "Clinical practice guidelines for the management of pain, agitation, and delirium in adult patients in the intensive care unit," *Crit Care Med*, vol. 41, 2013// 2013.
- [5] W. D. Schweickert and J. Hall, "ICU-acquired weakness," (in eng), *Chest*, vol. 131, no. 5, pp. 1541-9, May 2007.
- [6] S. M. Parry *et al.*, "Assessment of impairment and activity limitations in the critically ill: a systematic review of measurement instruments and their clinimetric properties," (in eng), *Intensive Care Med*, vol. 41, no. 5, pp. 744-62, May 2015.
- [7] A. Thrush, M. Rozek, and J. L. Dekkerlegand, "The Clinical Utility of the Functional Status Score for the Intensive Care Unit (FSS-ICU) at a Long-Term Acute Care Hospital: A Prospective Cohort Study," *Physical Therapy*, vol. 92, no. 12, pp. 1536-1545, 2012.
- [8] H. Brown, J. Terrence, P. Vasquez, D. W. Bates, and E. Zimlichman, "Continuous monitoring in an inpatient medical-surgical unit: a controlled clinical trial," (in eng), *Am J Med*, vol. 127, no. 3, pp. 226-32, Mar 2014.
- [9] E. Kipnis *et al.*, "Monitoring in the Intensive Care," *Critical Care Research and Practice*, vol. 2012, p. 20, 2012, Art. no. 473507.
- [10] K. B. To and L. M. Napolitano, "Common Complications in the Critically Ill Patient," *Surgical Clinics*, vol. 92, no. 6, pp. 1519-1557.
- [11] C. M. Wollschlager, A. R. Conrad, and F. A. Khan, "Common complications in critically ill patients," (in eng), *Dis Mon*, vol. 34, no. 5, pp. 221-93, May 1988.
- [12] H. B. Rubins and M. A. Moskowitz, "Complications of care in a medical intensive care unit," *Journal of General Internal Medicine*, journal article vol. 5, no. 2, pp. 104-109, March 01 1990.
- [13] S. V. Desai, T. J. Law, and D. M. Needham, "Long-term complications of critical care," (in eng), *Crit Care Med*, vol. 39, no. 2, pp. 371-9, Feb 2011.
- [14] M. Daily, S. Medasani, R. Behringer, and M. Trivedi, "Self-Driving Cars," *Computer*, vol. 50, no. 12, pp. 18-23, 2017.
- [15] J.-L. Vincent and J. Creteur, "Paradigm shifts in critical care medicine: the progress we have made," *Critical Care*, vol. 19, no. Suppl 3, pp. S10-S10, 12/18 2015.

- [16] W. Zhu, L. Jiang, S. Jiang, Y. Ma, and M. Zhang, "Real-time continuous glucose monitoring versus conventional glucose monitoring in critically ill patients: a systematic review study protocol," *BMJ Open*, 10.1136/bmjopen-2014-006579 vol. 5, no. 1, 2015.
- [17] L. J. Hirsch, "Continuous EEG Monitoring in the Intensive Care Unit: An Overview," *Journal of Clinical Neurophysiology*, vol. 21, no. 5, pp. 332-340, 2004.
- [18] N. S. Freedman, N. Kotzer, and R. J. Schwab, "Patient perception of sleep quality and etiology of sleep disruption in the intensive care unit," (in eng), *Am J Respir Crit Care Med*, vol. 159, no. 4 Pt 1, pp. 1155-62, Apr 1999.
- [19] E. W. Ely *et al.*, "Evaluation of delirium in critically ill patients: validation of the Confusion Assessment Method for the Intensive Care Unit (CAM-ICU)," *Critical care medicine*, vol. 29, no. 7, pp. 1370-1379, 2001.
- [20] D. Meagher *et al.*, "Development of an abbreviated version of the delirium motor subtyping scale (DMSS-4)," *International psychogeriatrics*, vol. 26, no. 4, pp. 693-702, 2014.
- [21] K. Zhang, Z. Zhang, Z. Li, and Y. Qiao, "Joint Face Detection and Alignment Using Multitask Cascaded Convolutional Networks," *IEEE Signal Processing Letters*, vol. 23, no. 10, pp. 1499-1503, 2016.
- [22] F. Schroff, D. Kalenichenko, and J. Philbin, "FaceNet: A unified embedding for face recognition and clustering," in *2015 IEEE Conference on Computer Vision and Pattern Recognition (CVPR)*, 2015, pp. 815-823.
- [23] C. Szegedy, S. Ioffe, V. Vanhoucke, and A. A. Alemi, "Inception-v4, Inception-ResNet and the Impact of Residual Connections on Learning," in *AAAI*, 2017, pp. 4278-4284.
- [24] B. Amos, B. Ludwiczuk, and M. Satyanarayanan, "OpenFace: A general-purpose face recognition library with mobile applications," in "CMU-CS-16-118," CMU School of Computer Science 2016.
- [25] C. C. Buckenmaier III, K. T. Galloway, R. C. Polomano, M. McDuffie, N. Kwon, and R. M. Gallagher, "Preliminary validation of the Defense and Veterans Pain Rating Scale (DVPRS) in a military population," *Pain Medicine*, vol. 14, no. 1, pp. 110-123, 2013.
- [26] Z. Cao, T. Simon, S.-E. Wei, and Y. Sheikh, "Realtime Multi-Person 2D Pose Estimation using Part Affinity Fields," *Computing Research Repository*, 2016.
- [27] I. J. Zaal *et al.*, "Intensive care unit environment may affect the course of delirium," *Intensive care medicine*, vol. 39, no. 3, pp. 481-488, 2013.
- [28] J. Patel, J. Baldwin, P. Bunting, and S. Laha, "The effect of a multicomponent multidisciplinary bundle of interventions on sleep and delirium in medical and surgical intensive care patients," *Anaesthesia*, vol. 69, no. 6, pp. 540-549, Jun 2014.
- [29] J. H. Han *et al.*, "Delirium in older emergency department patients: recognition, risk factors, and psychomotor subtypes," *Academic Emergency Medicine*, vol. 16, no. 3, pp. 193-200, 2009.
- [30] A. Godfrey, R. Conway, M. Leonard, D. Meagher, and G. O'laighin, "A classification system for delirium subtyping with the use of a commercial mobility monitor," *Gait & Posture*, vol. 30, no. 2, pp. 245-252, Aug 2009.
- [31] A. Godfrey, R. Conway, M. Leonard, D. Meagher, and G. M. O'laighin, "Motion analysis in delirium: A discrete approach in determining physical activity for the purpose of delirium motoric subtyping," *Medical Engineering & Physics*, vol. 32, no. 2, pp. 101-110, Mar 2010.
- [32] D. J. Meagher *et al.*, "Motor symptoms in 100 patients with delirium versus control subjects: comparison of subtyping methods," (in eng), *Psychosomatics*, vol. 49, no. 4, pp. 300-8, Jul-Aug 2008.
- [33] D. F. O'Connell, *Dual disorders: essentials for assessment and treatment*. Routledge, 2014.
- [34] B. K. Scott, "Disruption of Circadian Rhythms and Sleep in Critical Illness and its Impact on the Development of Delirium," *Current Pharmaceutical Design*, vol. 21, no. 24, pp. 3443-3452, 2015.
- [35] H. T. McKenna, I. K. Reiss, and D. S. Martin, "The significance of circadian rhythms and dysrhythmias in critical illness," *Journal of the Intensive Care Society*, vol. 18, no. 2, pp. 121-129, 2017.



- [36] C. J. Madrid-Navarro *et al.*, "Disruption of Circadian Rhythms and Delirium, Sleep Impairment and Sepsis in Critically ill Patients. Potential Therapeutic Implications for Increased Light-Dark Contrast and Melatonin Therapy in an ICU Environment," *Current Pharmaceutical Design*, vol. 21, no. 24, pp. 3453-3468, 2015.
- [37] D. McDuff, R. E. Kalioubi, K. Kassam, and R. Picard, "Affect valence inference from facial action unit spectrograms," in *2010 IEEE Computer Society Conference on Computer Vision and Pattern Recognition - Workshops*, 2010, pp. 17-24.
- [38] A. B. Cooke, S. S. Daskalopoulou, and K. Dasgupta, "The impact of accelerometer wear location on the relationship between step counts and arterial stiffness in adults treated for hypertension and diabetes," (in eng), *J Sci Med Sport*, Aug 24 2017.
- [39] M. E. Rosenberger, W. L. Haskell, F. Albinali, S. Mota, J. Nawyn, and S. Intille, "Estimating Activity and Sedentary Behavior From an Accelerometer on the Hip or Wrist," *Medicine and science in sports and exercise*, vol. 45, no. 5, pp. 964-975, 2013.
- [40] A. H. K. Montoye, J. M. Pivarnik, L. M. Mudd, S. Biswas, and K. A. Pfeiffer, "Validation and Comparison of Accelerometers Worn on the Hip, Thigh, and Wrists for Measuring Physical Activity and Sedentary Behavior," *AIMS Public Health*, vol. 3, no. 2, pp. 298-312, 2016.
- [41] T. C. Araújo and L. W. S. da Silva, "Music: a care strategy for patients in intensive care unit," *Journal of Nursing UFPE on line*, vol. 7, no. 5, pp. 1319-1325, 2013.
- [42] G. O'Malley, M. Leonard, D. Meagher, and S. T. O'Keeffe, "The delirium experience: a review," (in eng), *J Psychosom Res*, vol. 65, no. 3, pp. 223-8, Sep 2008.
- [43] G. Mistraletti, P. Pelosi, E. S. Mantovani, M. Berardino, and C. Gregoretti, "Delirium: clinical approach and prevention," (in eng), *Best Pract Res Clin Anaesthesiol*, vol. 26, no. 3, pp. 311-26, Sep 2012.
- [44] A. Granberg, I. B. Engberg, and D. Lundberg, "Intensive care syndrome: a literature review," *Intensive and Critical Care Nursing*, vol. 12, no. 3, pp. 173-182, 1996.
- [45] B. Van Rompaey, A. Van Hoof, P. van Bogaert, O. Timmermans, and T. Dilles, "The patient's perception of a delirium: A qualitative research in a Belgian intensive care unit," *Intensive and Critical Care Nursing*, vol. 32, no. Supplement C, pp. 66-74, 2016/02/01/ 2016.
- [46] E. Sprague, S. Reynolds, and P. G. Brindley, "Patient isolation precautions: Are they worth it?," (in eng), *Can Respir J*, Nov 5 2015.
- [47] R. G. Rosa *et al.*, "Effectiveness and Safety of an Extended ICU Visitation Model for Delirium Prevention: A Before and After Study\*," *Critical Care Medicine*, vol. 45, no. 10, pp. 1660-1667, 2017.
- [48] J. E. Sasaki, D. John, and P. S. Freedson, "Validation and comparison of ActiGraph activity monitors," *Journal of Science and Medicine in Sport*, vol. 14, no. 5, pp. 411-416, 2011.
- [49] P. Ekman and W. V. Friesen, *Manual for the facial action coding system*. Consulting Psychologists Press, 1978.
- [50] P. Lucey *et al.*, "Automatically detecting pain in video through facial action units," *IEEE Transactions on Systems, Man, and Cybernetics, Part B (Cybernetics)*, vol. 41, no. 3, pp. 664-674, 2011.
- [51] J. Long, E. Shelhamer, and T. Darrell, "Fully convolutional networks for semantic segmentation," in *Proceedings of the IEEE Conference on Computer Vision and Pattern Recognition*, 2015, pp. 3431-3440.
- [52] C. J. Tipping *et al.*, "The ICU Mobility Scale has construct and predictive validity and is responsive. A multicenter observational study," *Annals of the American Thoracic Society*, vol. 13, no. 6, pp. 887-893, 2016.
- [53] W. L. Titsworth *et al.*, "The effect of increased mobility on morbidity in the neurointensive care unit," *Journal of neurosurgery*, vol. 116, no. 6, pp. 1379-1388, 2012.
- [54] N. R. Council, *Hearing loss: Determining eligibility for social security benefits*. National Academies Press, 2004.

- [55] G. Associates. (4/19/2018). *Acoustic Glossary*. Available: <http://www.acoustic-glossary.co.uk/sound-pressure.htm>
- [56] (2016, 4/19/2018). *Lux Measurements*. Available: <https://actigraph.desk.com/customer/en/portal/articles/2515504-lux-measurements>
- [57] H. Wang, X. Liang, H. Zhang, D.-Y. Yeung, and E. P. Xing, "ZM-Net: Real-time Zero-shot Image Manipulation Network," *arXiv preprint arXiv:1703.07255*, 2017.
- [58] P. F. Felzenszwalb, R. B. Girshick, D. McAllester, and D. Ramanan, "Object Detection with Discriminatively Trained Part-Based Models," *IEEE Transactions on Pattern Analysis and Machine Intelligence*, vol. 32, no. 9, pp. 1627-1645, 2010.
- [59] K. Q. Weinberger and L. K. Saul, "Distance metric learning for large margin nearest neighbor classification," *Journal of Machine Learning Research*, vol. 10, no. Feb, pp. 207-244, 2009.
- [60] G. B. Huang, M. Ramesh, T. Berg, and E. Learned-Miller, "Labeled faces in the wild: A database for studying face recognition in unconstrained environments," Technical Report 07-49, University of Massachusetts, Amherst 2007.
- [61] P. F. Felzenszwalb and D. P. Huttenlocher, "Pictorial structures for object recognition," *International journal of computer vision*, vol. 61, no. 1, pp. 55-79, 2005.
- [62] G. Papandreou *et al.*, "Towards Accurate Multi-person Pose Estimation in the Wild," *arXiv preprint arXiv:1701.01779*, 2017.
- [63] M. Sun and S. Savarese, "Articulated part-based model for joint object detection and pose estimation," presented at the Computer Vision (ICCV), 2011 IEEE International Conference on, 2011.
- [64] K. Simonyan and A. Zisserman, "Very deep convolutional networks for large-scale image recognition," *arXiv preprint arXiv:1409.1556*, 2014.
- [65] L. Pishchulin, A. Jain, M. Andriluka, T. Thormählen, and B. Schiele, "Articulated people detection and pose estimation: Reshaping the future," in *2012 IEEE Conference on Computer Vision and Pattern Recognition*, 2012, pp. 3178-3185.
- [66] O. Troyanskaya *et al.*, "Missing value estimation methods for DNA microarrays," (in eng), *Bioinformatics*, vol. 17, no. 6, pp. 520-5, Jun 2001.

## Appendix A.

Sleep in the Intensive Care Unit (ICU) Questionnaire:

1. Rate the overall quality of your sleep at home. 1 2 3 4 5 6 7 8 9 10  
Use a scale of 1 to 10 (1 is poor, 10 is excellent)
2. Rate the overall quality of your sleep in the ICU. 1 2 3 4 5 6 7 8 9 10  
Use a scale of 1 to 10 (is poor, 10 is excellent)
3. Rate the overall quality of your sleep in the ICU on the following days:  
(1 is poor, 10 is excellent)
  - On the first night in the ICU 1 2 3 4 5 6 7 8 9 10
  - During the middle of your ICU stay 1 2 3 4 5 6 7 8 9 10
  - At the end of your ICU stay 1 2 3 4 5 6 7 8 9 10
4. Rate the overall degree of daytime sleepiness during your ICU stay: 1 2 3 4 5 6 7 8 9 10  
(1 is unable to stay awake, 10 is fully alert and awake)
5. Rate the overall degree of daytime sleepiness during your ICU stay on the following days:

- (1 is unable to stay awake, 10 is fully alert and awake)
- On the first night in the ICU 1 2 3 4 5 6 7 8 9 10
  - During the middle of your ICU stay 1 2 3 4 5 6 7 8 9 10
  - At the end of your ICU stay 1 2 3 4 5 6 7 8 9 10
6. Rate how disruptive the following activities were to your sleep during your ICU stay.  
Use a scale of 1 to 10. (1 is no disruption, 10 is significant disruption)
- Noise 1 2 3 4 5 6 7 8 9 10
  - Light 1 2 3 4 5 6 7 8 9 10
  - Nursing interventions (i.e. baths) 1 2 3 4 5 6 7 8 9 10
  - Diagnostic Testing (i.e. chest x-rays) 1 2 3 4 5 6 7 8 9 10
  - Vital Signs (blood pressure, pulse, temperature) 1 2 3 4 5 6 7 8 9 10
  - Blood Samples 1 2 3 4 5 6 7 8 9 10
  - Administration of Medications 1 2 3 4 5 6 7 8 9 10
7. Rate how disruptive the following noises were to your sleep during your ICU stay.  
(1 is no disruption, 10 is significant disruption)
- Heart Monitor Alarm 1 2 3 4 5 6 7 8 9 10
  - Ventilator Alarm 1 2 3 4 5 6 7 8 9 10
  - Ventilator 1 2 3 4 5 6 7 8 9 10
  - Oxygen Finger Probe 1 2 3 4 5 6 7 8 9 10
  - Talking 1 2 3 4 5 6 7 8 9 10
  - I.V. Pump Alarm 1 2 3 4 5 6 7 8 9 10
  - Suctioning 1 2 3 4 5 6 7 8 9 10
  - Nebulizer 1 2 3 4 5 6 7 8 9 10
  - Doctor's Beepers 1 2 3 4 5 6 7 8 9 10
  - Television 1 2 3 4 5 6 7 8 9 10
  - Telephone 1 2 3 4 5 6 7 8 9 10

## Appendix B.

### Face Detection

To detect individual faces, we extracted seven seconds of still images at 15 fps as training data and used the Joint Face Detection and Alignment using Multi-Task Cascaded Convolutional Network (MTCNN). This framework employs a cascaded architecture with three stages of deep convolutional neural networks (CNN) to predict face and landmark locations in a coarse-to-fine manner. In the first stage, candidate windows possibly containing faces are produced using a fully convolutional network called Proposal Network (P-Net) (Figure 2.a, Supplement) [57]. Each candidate window has four coordinates – top left coordinates, height, and width. Ground truth bounding boxes have the same coordinate format as well. The objective function for bounding box regression performed on these candidate windows is Euclidean loss between the corresponding coordinates of a candidate window and its nearest ground truth bounding box. The objective is to minimize this Euclidean loss, given for a sample  $x_i$  as in Eq. 3.

$$L_i^{box} = \|\hat{y}_i^{box} - y_i^{box}\|_2^2 \quad (3)$$

Here,  $\hat{y}_i^{box}$  is the output regression coordinate obtained from the network and  $y_i^{box}$  is the ground-truth coordinate. After performing bounding box regression, the highly overlapping candidates are merged using non-maximum suppression (NMS) [58]. NMS is performed by sorting the bounding boxes by their score, and greedily selecting the highest scoring boxes and removing the boxes that overlap with the already selected boxes more than a given threshold, 0.7 in the first stage. In the second stage, all candidates selected in the first stage are provided to another convolutional network, Refine Network (R-Net) (Figure 2.b, Supplement). R-Net further rejects candidate windows not containing faces, performs bounding box regression, and merges the NMS candidates with threshold of 0.7. Finally, the Output Network (O-Net) produces the final bounding box (Figure 2.c, Supplement). MTCNN is trained for bounding box regression

by posing its objective function as a regression problem. While extracting the candidate windows during testing, a window is selected on the basis of the threshold given for Intersection over Union (IoU) score, calculated as in Eq. 4.

$$IoU_i = \frac{A_i^o}{A_i^u} \quad (4)$$

Here,  $A_i^o$  is the area of overlap between the  $i$ th ground-truth bounding box and the  $i$ th detected bounding box, and  $A_i^u$  is the area of union between the  $i$ th ground-truth bounding box and the  $i$ th detected bounding box. If the  $IoU_i$  is above the given threshold for a candidate window, the window is selected for the next stage. The three-stage threshold values used for selecting the candidate windows were 0.6, 0.7 and 0.9 respectively. The face thumbnails obtained from this framework have a size of 160\*160 pixels. These thumbnails are provided to the face recognition framework as input.

### Face Recognition

FaceNet is a deep CNN model that extracts facial features in terms of 128-D Euclidean (L2) embeddings using a triplet-based loss function [59]. The input to FaceNet model is the set of aligned images obtained from MTCNN. The network is trained such that the squared L2 distances in the embedding space directly correspond to face similarity. These embedding vectors can then be used as feature vectors for a classification model. We used the FaceNet model pre-trained on a subset of MS-celeb-1M dataset which includes about 10 million images of 100,000 celebrities [23], which had an accuracy of 0.99 on the Labeled Faces in the Wild (LFW) dataset [60]. The pre-trained model was used to extract features from patient thumbnails and to calculate the corresponding L2 embeddings for our training images. These embeddings are then used to train a linear Support Vector Machine (SVM) for classification, on a fixed number of images ( $n=100$ , ~ 7 seconds of video) of a patient, along with the same number of negative examples of non-patients. The tolerance value for stopping criterion was set to 0.001.

### Appendix C.

#### Posture Classification

While our recorded patient frames contain examples of functional status activities such as walking, sitting in bed, or sitting in chair, these activities are interspersed in an imbalanced and sparse manner throughout the video clips. To remedy this problem, besides patient data, we additionally recorded 90 minutes of video containing scripted functional activities performed by actors in the same ICU rooms. Out of the 150,621 video frames, 74,924 frames are scripted, and 75,697 frames are taken based on actual ICU patients' videos.

The initial size of each frame was 1680x1050, which was reduced to 368x654 to accommodate the memory. We used a multi-person pose estimation model [26] to localize anatomical key-points of joints and limbs. Most algorithms are single-person estimators [61-63], such that they first detect each person and then estimate the location of joints and limbs. The single-person approach suffers from early commitment problem when multiple people are in close proximity; if an incorrect detection is made initially, there is no point of return as this approach tracks the initial detection. Due to the small size of hospital rooms and presence of multiple people (patient, doctors, nurses, visitors), we used the multi-person approach [26]. It also allows us to decouple the runtime complexity from the number of people for real-time implementations. The multi-person pose estimation was performed using the real-time multi-person 2D pose estimation with part affinity fields. The part affinity fields are 2D vector fields that contain information about the location and direction of limbs with respect to body joints. Our pose detection model consists of two branches of a sequential prediction process, where one branch detects the locations of joints, and the other branch detects the association of those body joints, as limbs. Both branches consist of Fully Convolutional Neural networks (FCN) [51]. A convolutional network, consisting of first 10 layers of VGG-19 [64], is used to generate a set of feature maps  $\mathbf{F}$ . These feature maps are used as input to each branch of the first stage of the model. The first branch outputs a set of detection confidence maps  $S^1 = \rho^1(\mathbf{F})$  and

the second branch outputs a set of part affinity fields  $L^1 = \phi^1(F)$  where  $S^1$  and  $\phi^1$  are the two branches of CNNs at the first stage. In the following stage, the outputs from the branches in the previous stage and the original image features  $F$  are combined and provided as inputs to the two branches of the next stage, for further refinement. The confidence maps and part affinity fields for the subsequent stages are calculated as in Eq. 5 and Eq. 6, respectively [26].

$$S^t = \rho^t(F, S^{t-1}, L^{t-1}), \forall t \geq 2 \quad (5)$$

$$L^t = \phi^t(F, S^{t-1}, L^{t-1}), \forall t \geq 2 \quad (6)$$

This process is followed for the  $t$  stages of the network. We have used three stages of the network in our model.

This model has been pre-trained on the MPII Human Pose dataset for 144,000 iterations. It contains over 40K activities with annotated body joints [65]. The final model provided a state-of-the-art mean average precision of 0.79 on MPII dataset. We used the lengths of body limbs and their relative angles as features for the classification model. We used estimated poses to detect the four functional activities. We got the best results with K-Nearest Neighbors for classification, with Minkowski distance metric and value of K equal to one.

During the poselet detection step, sometimes a few anatomical key-points were not detected. This led to the problem of missing values for some features in the data that were provided to the classification model. Most algorithms are not immune to missing values. Several methods can be used to impute missing values, including mean, median, mode, or amputation via k-nearest neighbors (k-NN) [66]. The K nearest neighbors are found based on the distance with the remaining features between the different samples. Each missing value of a feature was imputed by the weighted average of the same feature of the k nearest neighbors, with a K value of three. The resulting poselets were then used to train and test the classification algorithm on our dataset. We used 80% of our data for training, and 20% for training. The ICU training data included 74,924 frames from the scripted dataset and 75,697 frames from the actual ICU patients. Test data comprised only actual patient data. The hyper-parameters of the classification algorithms were fine-tuned using GridSearchCV with five-fold cross-validation. Pipeline of posture recognition model is shown in Figure 5.b.

## Supplement Figures/Tables

### Cohort Summary

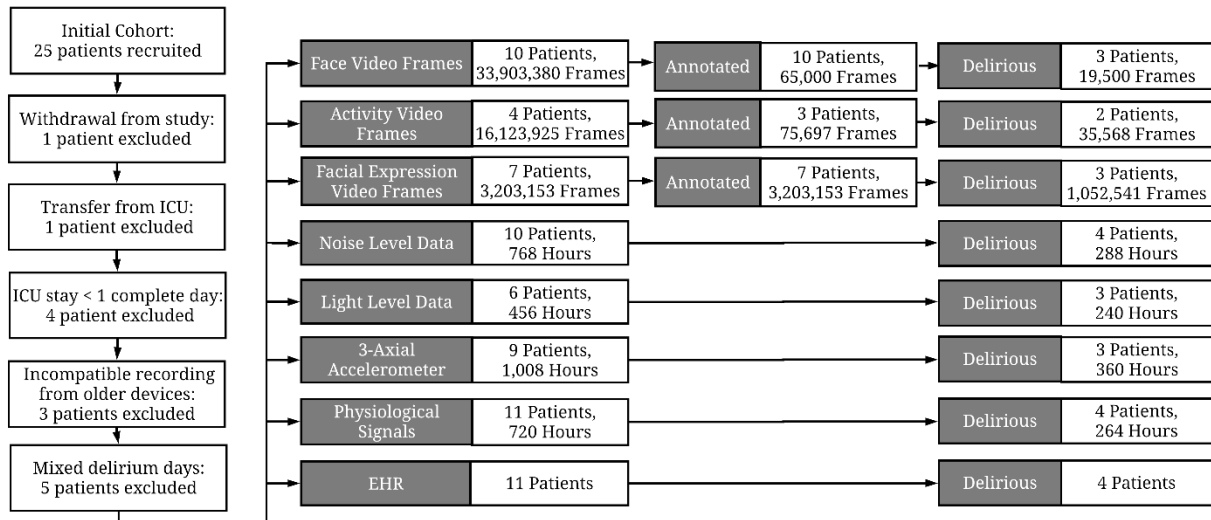


Figure 1. Cohort recruitment diagram.

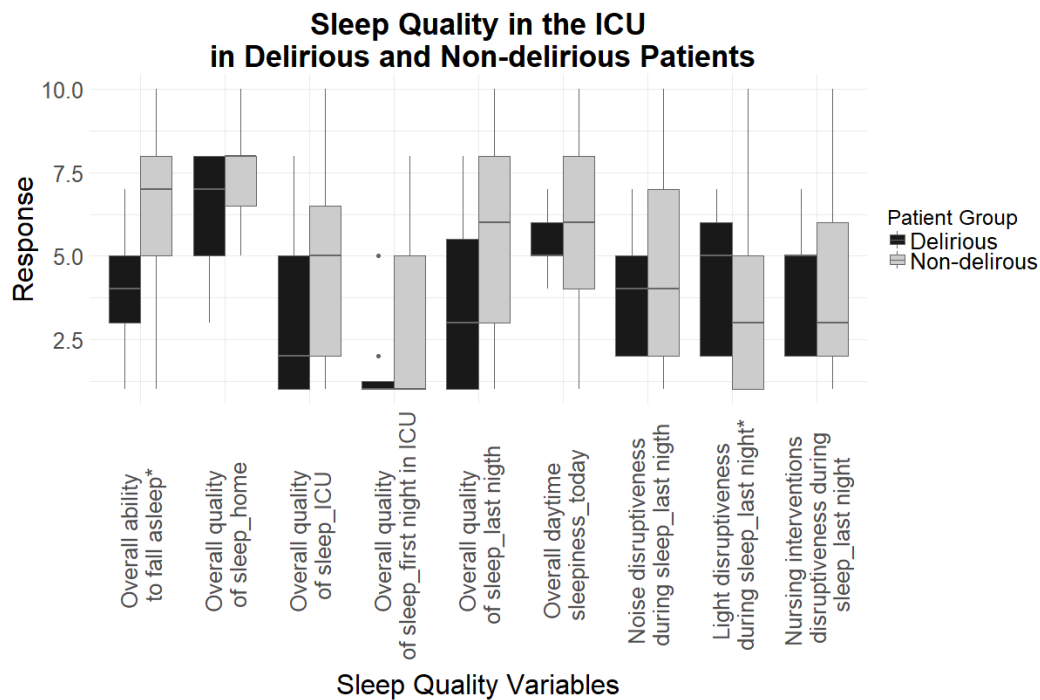


Figure 2. Sleep quality outcomes, patient self-reports using Freedman Sleep Questionnaire. The parameters range from 1 to 10, with 1 being poor and 10 being excellent for the first five criteria. For overall daytime sleepiness, 1 is unable to stay awake, 10 is fully alert and awake. For environment and nursing interventions disruptiveness variables, 1 is no disruption, 10 is significant disruption. \*: p-value less than 0.05. Number of delirium nights: 9. Number of non-delirium nights: 43.

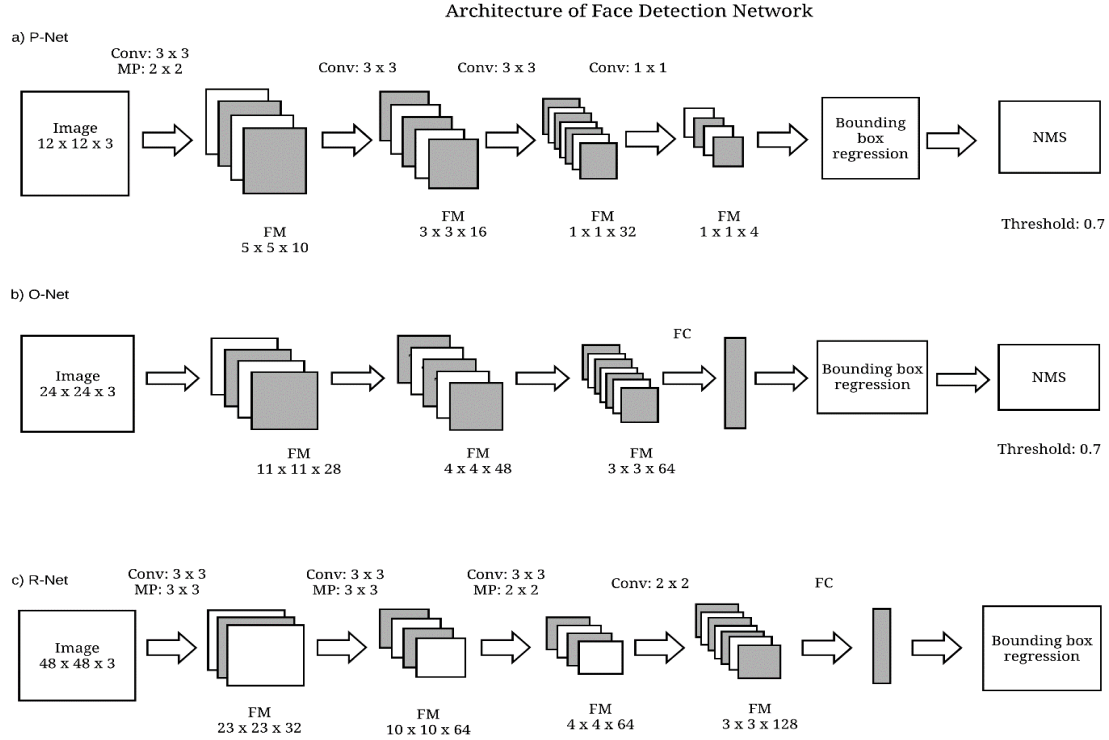


Figure 3. Architectures of P-Net, R-Net and O-Net. Conv: Convolutional, MP: Max pooling, FC: Fully Connected layer, FM: Feature Maps and NMS: Non-Maximum Suppression. The numbers denote the kernel size in Conv and MP layers. The numbers for FM denote the height, width and depth of the FM. The step-size for each Conv layer is one and for each MP layer is two.

Table 1 List of Electronic Health Records variables included in the study. N= Number of days.

Variable, median (25 <sup>th</sup> , 75 <sup>th</sup> )	Non-delirious (N=42)	Delirious (N=17)	p-value
<b>Physiological</b>			
- Heart rate	87.0 (76.0, 101.0)	90.0 (79.0, 99.0)	0.31
- Systolic blood pressure	129.0 (117.0, 141.25)	114.0 (105.0, 127.0)	<0.01
- Diastolic blood pressure	72.5 (61.0, 81.0)	62.0 (56.0, 71.7)	<0.01
- Respiration rate	20.0 (17.0, 23.0)	22.0 (18.0, 25.0)	<0.01
- SPO2	97.0 (95.0, 99.0)	99.0 (97.0, 100.0)	<0.01
- Body temperature	98.0 (97.3, 98.6)	99.3 (98.8, 99.9)	<0.01

Table 2. Action Units (AUs) for each facial expression. AU1: Inner brow raiser, AU2: Outer brow raiser, AU4: Brow lowerer, AU5: Upper lid raiser, AU6: cheek raiser, AU7: Lid tightener, AU9: Nose wrinkle, AU10: Upper lip raiser, AU12: Lip corner puller, AU14: Dimpler, AU15: Lip corner depressor, AU16: Lower lip depressor, AU20: Lip stretcher, AU23: Lip tightener, AU26: Jaw drop, AU43: Eyes closed. There are other modifiers for facial AUs: "R" represents an action that occurs on the right side, and an action that is unilateral but has a stronger side is indicated with an "A" [49, 50]. Only AUs detected by OpenFace toolbox were used and are reported in bold in the table.

Facial Expression	AUs
<b>Happiness</b>	<b>6+12</b>
<b>Sadness</b>	<b>1+4+15</b>
<b>Surprise</b>	<b>1+2+5+26</b>
<b>Fear</b>	<b>1+2+4+5+7+20+26</b>
<b>Anger</b>	<b>4+5+7+23</b>
<b>Disgust</b>	<b>9+15+16</b>
<b>Contempt</b>	<b>R12A+R14A</b>
<b>Pain</b>	<b>4+6  7+9  10+43</b>

Table 3. Confusion matrix showing the model performance for the four postures -lying, sitting on bed, sitting on chair, and standing- using K-Nearest Neighbor model. Correct detections are presented in bold. Due to random frame selection, there was no frame with the patient sitting in bed in the annotated dataset.

		Predicted label		
True label		Lying	Sitting on chair	Standing
	Lying	<b>94.45</b>	0.79	4.76
	Sitting on chair	1.73	<b>92.89</b>	5.38
	Standing	4.23	11.97	<b>83.8</b>

Table 4. BRADEN scale scores for delirious, non-delirious and all patient scores. N: Number of observations, each category ranges from 1-4, except for “friction and shear” which is 1-3. Higher scores mean less risk of developing pressure ulcer. Sensory perception reflects ability to respond meaningfully to pressure-related discomfort, moisture is about degree to which skin is exposed to moisture, activity is about degree of physical activity, mobility is about ability to change and control body position, nutrition is about usual food intake pattern, and friction and shear is about requiring help to move.

	All (N=131)	Delirious (N=32)	Non-delirious (N=99)	P-value
<b>Braden Sensory Perception, median</b>	3 (3-4)	3.5 (2.75-4)	3 (3-4)	0.82
<b>Braden Moisture, median (IQR)</b>	3 (3-3)	3 (3-3)	3 (3-3)	0.73
<b>Braden Activity, median (IQR)</b>	2 (1-3)	2 (1-2.25)	2 (1-3)	<b>0.02</b>
<b>Braden Mobility, median (IQR)</b>	3 (2-3)	3 (2.75-3)	2 (2-3)	<b>0.01</b>
<b>Braden Nutrition, median (IQR)</b>	2 (2-3)	2 (2-3)	2 (2-3)	0.69
<b>Braden Friction &amp; Shear, median (IQR)</b>	2 (2-2)	2 (2-2)	2 (1.5-2)	<b>&lt;0.001</b>
<b>Braden Score, median (IQR)</b>	16 (13-17)	16 (14.25-16.25)	15 (13-17)	0.84

Table 5 Examples of sound pressure and sound pressure levels.

Sources at 1 m	Sound Pressure	SPL (reference sound pressure=0dB)
<b>Threshold of pain</b>	20 Pa	120 dB
<b>Pneumatic hammer</b>	2 Pa	100 dB
<b>Street traffic</b>	0.2 Pa	80 dB
<b>Talking</b>	0.02 Pa	60 dB
<b>Library</b>	0.002 Pa	40 dB
<b>TV Studio</b>	0.0002 Pa	20 dB
<b>Threshold of hearing</b>	0.00002 Pa	0 dB

Table 6 Estimate of industry accepted lux values.

Lux Level	Interpretation Comparison
<b>1</b>	Twilight
<b>5</b>	Minimal Street Lighting
<b>10</b>	Sunset
<b>50</b>	Family Living Room
<b>80</b>	Hallway
<b>100</b>	Very Dark Overcast Day
<b>320-500</b>	Office Lighting
<b>400</b>	Sunrise/Sunset
<b>1,000</b>	Overcast Day
<b>10,000-25,000</b>	Full Daylight



Table 7. Actigraphy features for the **arm**, comparing between the delirious and non-delirious groups. M10: activity level during the 10-hour window with the highest sum of activity, L5: activity level during the 5-hour window with the lowest sum of activity. Relative amplitude:  $(M10-L5)/(M10+L5)$ . RMSSD: Root mean square of sequential differences. RMSSD/SD: root mean square of sequential differences/standard deviation. Immobile minutes are minutes with zero activity.

	Non-delirium(N=15)	Delirium (N=3)	p-value
Mean of activity for whole day, median (IQR)	25.6 (13.6, 125.9)	4.8 (3.2, 15.2)	0.10
Mean of activity for daytime	33.9 (11.8, 126.9)	6.7 (4.5, 11.9)	0.08
SD of activity for daytime	139.1 (71.6, 370.1)	54.3 (43, 84.8)	0.08
Mean of activity for nighttime	21.8 (8.9, 66.1)	0 (0, 19.8)	0.15
SD of activity for nighttime	103.4 (58.1, 296.2)	0 (0, 70.9)	0.12
M10	30081.5 (13732.6, 147613.8)	6841.1 (4636.5, 13373.4)	0.06
Time of M10	317 (162, 548)	413 (241.5, 545.5)	0.82
Time of M10 (hour)	6 (3, 9.5)	7 (4.5, 8)	0.81
L5	927.5 (593.4, 2789.8)	0 (0, 252.7)	<b>0.04</b>
Time of L5	400 (132, 1028)	1 (1, 211)	0.15
Time of L5 (hour)	7 (2.5, 18)	1 (1, 4.5)	0.19
RA	0.9 (0.9, 1)	1 (0.97, 1)	0.06
SD of activity for whole day	106.6 (84.5, 346.1)	81.6 (52, 95)	0.20
RMSSD	117.6 (103.1, 360.7)	85.6 (56.7, 102.8)	0.20
RMSSD/SD	1.1 (1, 1.2)	1.1 (1.1, 1.2)	0.57
Number of immobile minutes during the day	589 (498.5, 670.5)	683 (636.5, 697)	0.16
Number of immobile minutes during the night	632 (601.5, 673)	720 (605, 720)	0.29

Table 8. Actigraphy features for the **ankle**, comparing between the delirious and non-delirious groups. M10: activity level during the 10-hour window with the highest sum of activity, L5: activity level during the 5-hour window with the lowest sum of activity. Relative amplitude:  $(M10-L5)/(M10+L5)$ . RMSSD: Root mean square of sequential differences. RMSSD/SD: root mean square of sequential differences/standard deviation. Immobile minutes are minutes with zero activity.

	Non-delirium (N=15)	Delirium (N=5)	p-value
Mean of activity for whole day, median (IQR)	8 (7.1, 27.1)	12.6 (7.2, 20.6)	0.79
Mean of activity for daytime	8.9 (6.6, 28.3)	9.1 (8.6, 25.4)	0.79
SD of activity for daytime	61.7 (57.2, 98.7)	59.1 (52.2, 61.6)	0.54
Mean of activity for nighttime	9.8 (5.3, 22.4)	20.6 (4, 24.2)	0.86
SD of activity for nighttime	64.6 (42.2, 80.2)	54.4 (24.6, 69.2)	0.73
M10	8094.1 (6817.2, 27183.4)	16149.2 (8094.1, 21255.3)	0.43
Time of M10	315 (129.5, 475.5)	384 (72, 614)	0.93
Time of M10 (hour)	6 (2.5, 8.5)	7 (2, 11)	0.93
L5	544.4 (287.6, 2067.1)	588.5 (544.4, 1864.4)	0.60
Time of L5	722 (47, 933.5)	894 (299, 1083)	0.54
Time of L5 (hour)	13 (1.5, 16)	15 (5, 19)	0.54
RA	0.9 (0.9, 0.9)	0.9 (0.8, 0.9)	0.34
SD of activity for whole day	61.4 (52.3, 91.2)	49.8 (45, 65.6)	0.54
RMSSD	75.6 (66.6, 109.9)	50.2 (50.1, 70.5)	0.26
RMSSD/SD	1.2 (1.1, 1.3)	1.1 (1.1, 1.1)	<b>0.03</b>
Number of immobile minutes during the day	650 (529.5, 686)	645 (557, 650)	0.57
Number of immobile minutes during the night	673 (544.5, 690.5)	559 (525, 673)	0.34